

## Heating of $\text{Al}_{13}^-$ and $\text{Al}_{14}$ clusters

Jaakko Akola\* and Matti Manninen

*Department of Physics, University of Jyväskylä, FIN-40351 Jyväskylä, Finland*

(Received 15 January 2001; published 30 April 2001)

Dynamical properties of  $\text{Al}_{13}^-$  and  $\text{Al}_{14}$  clusters at a high-temperature regime are studied using a density functional theory based first-principles simulations method. During the heating  $\text{Al}_{13}^-$  shows a significantly different behavior than  $\text{Al}_{14}$  due to its double-magic nature. We also demonstrate that it is hard to assign any distinct melting transition for the studied cluster sizes. For  $\text{Al}_{13}^-$  we observe a solidlike behavior well after the melting temperature of bulk aluminum. In contradiction with the rare gas clusters we notice that the outermost atom of icosahedral  $\text{Al}_{14}$  does not float around when the temperature is increased. Instead the whole cluster will exhibit strong deformations. The electronic structure of both of the clusters shows strong fluctuations during the heatings, which cause considerable broadening and smearing effects in the electronic spectra.

DOI: 10.1103/PhysRevB.63.193410

PACS number(s): 36.40.Cg, 36.40.Mr, 73.22.-f

Atomic clusters as intermediate objects between single atoms and bulk matter have attracted scientists during the last decades. The emergence of spherical jellium model straightly analogous to the historical nuclear shell model and its implications on the physical properties of clusters have raised especially metal clusters in the forefront of contemporary cluster research.<sup>1,2</sup> Similarly, studies on the dynamical properties of atomic clusters have revealed new kinds of ‘‘phases’’ or existence forms where the system can remain for considerable time scales.<sup>3</sup> Furthermore, due to their finite size clusters do not exhibit sharp phase transitions in the conventional sense,<sup>4,5</sup> and related, several observations have been made where clusters of certain sizes exhibit a well-defined equilibrium between their coexisting solid and liquid forms.<sup>5-9</sup> In addition, also other dynamically interesting properties such as, e.g., cluster growth,<sup>10,11</sup> diffusion mechanisms on clusters,<sup>11</sup> solid-to-solid transitions,<sup>12,13</sup> and surface melting have been reported.<sup>14-16</sup>

For computational reasons, dynamical properties and the related phase diagrams of clusters have been mostly studied using simple classical potentials (e.g., Lennard-Jones) where the detailed electronic structure of the cluster is neglected. Although we are still far from the exhaustive first-principles sampling of the phase space of clusters, some simulations where the electronic structure is fully taken into account have already been successfully performed for small Na clusters<sup>17</sup> in comparison with the experimental temperature-dependent photoabsorption experiments.<sup>18</sup> In this communication, we report our findings on first-principles heating simulations of  $\text{Al}_{13}^-$  and  $\text{Al}_{14}$  clusters, and we shall further show that this approach has its justification among the conventional many-atom potentials. While these classical potentials describe well the melting of bulk metals<sup>19</sup> and metal surfaces<sup>20</sup> they cannot describe the salient effects caused by the electronic shell structure in small clusters. The motivation to study the particular  $\text{Al}_{13}^-$  and  $\text{Al}_{14}$  clusters (40 and 42 valence electrons, respectively) is that the first one as a 13-atom icosahedron (ICS) is ‘‘double magic’’ (i.e., it has both full atom and electron shells) while the latter represents a new shell opening in both respects.<sup>21,22</sup> The current paper is an extension of our earlier work<sup>21,22</sup> and we focus here on the high-temperature properties of these clusters.

The calculations are performed using a so called Born-Oppenheimer local-spin-density molecular dynamics (BO-LSD-MD) simulation method devised by Barnett and Landman and fully documented in Ref. 24. In this method the valence electron density is evaluated using a plane wave basis set, separable nonlocal norm-conserving pseudopotentials,<sup>25</sup> and the density functional Kohn-Sham (KS) method where the exchange-correlation energy functional is described by the LSD approximation.<sup>26</sup> During molecular dynamics and possible optimization, the ions move on the Born-Oppenheimer potential energy surface, where the classical Hellmann-Feynman forces on ions are calculated from the converged solution of valence electron density. The usage of the BO approximation allows a relatively large time step,  $\tau \approx 1 - 10$  fs, for the integration of the ionic equations of motion, the limiting time scale arising from the real ion dynamics (characteristic frequencies). In this work, the heating simulations of  $\text{Al}_{13}^-$  and  $\text{Al}_{14}$  have been performed by linearly scaling the kinetic energy of ions during the microcanonical molecular dynamics ( $\tau = 5$  fs). For practical reasons a heating rate of 10 K/ps had to be used in order to obtain the desired amount of data. We remark in this context that the relatively rapid heating of clusters makes true equilibrium unattainable. In the following, our results consist of one heating run for both  $\text{Al}_{13}^-$  and  $\text{Al}_{14}$  where the temperature ranges are 800–1600 K and 700–1100 K corresponding to 80 ps and 40 ps simulation times, respectively.

The potential energies (per atom) of  $\text{Al}_{13}^-$  and  $\text{Al}_{14}$  during the heating simulations are displayed in Fig. 1 together with some snapshots of cluster geometries corresponding to local potential energy maxima. The initial configurations for both of the simulations were icosahedral geometries (based on a 13-atom ICS), which were stochastically thermalized before the actual heating simulation was started. Immediately, it is observed that it is impossible to assign any distinct transition (melting) regions in the data, which is not surprising due to the small size of the clusters. Both of the simulations show oscillating patterns which for  $\text{Al}_{13}^-$  are disturbed by occasional isomerization peaks (behavior similar to a  $\text{Na}_8$  cluster<sup>17</sup>). These peaks start to dominate the data in the high-temperature limit ( $\sim 1500$  K), indicating a molten phase behavior. It is apparent that  $\text{Al}_{14}$  does not show fluctuations as

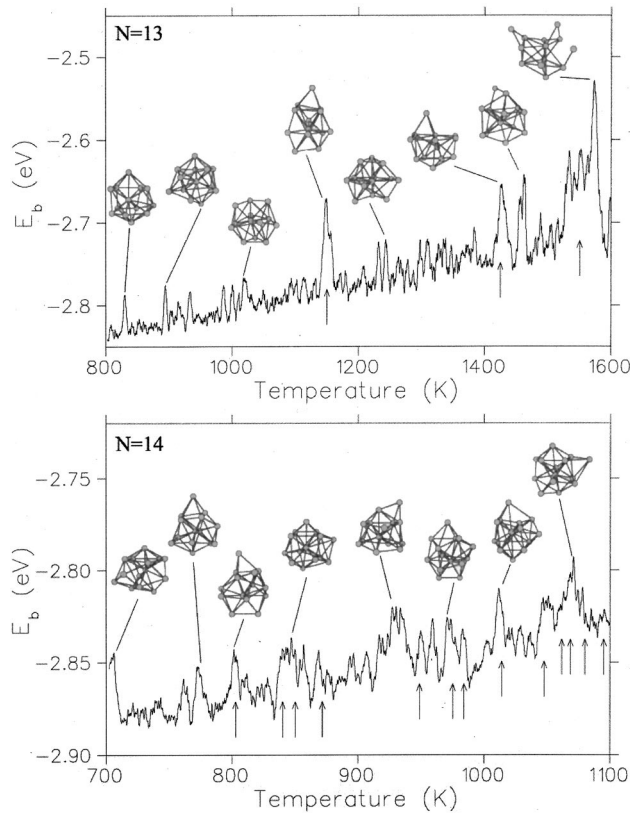


FIG. 1. The potential energies per atom of  $\text{Al}_{13}^-$  and  $\text{Al}_{14}$  clusters as a function of cluster temperature (averaged kinetic energy). The snapshots of cluster geometries represent the isomerization peaks. Arrows mark the positions where the central atom of  $\text{Al}_{13}^-$  and the outermost atom of  $\text{Al}_{14}$  are exchanged, respectively. Note the different energy scales of  $\text{Al}_{13}^-$  and  $\text{Al}_{14}$  data.

strong but, as discussed in the following, we do not believe that this is caused solely by the smaller temperature range than in the case of  $\text{Al}_{13}^-$ .

During the low-temperature parts of the heating simulations we observe that the icosahedral ground state geometries together with the corresponding decahedral ones are the prevailing structures. Especially for  $\text{Al}_{14}$ , the decahedron (DC) is preferable at a finite temperature due to its (100) facets where the outermost atom can sit tightly. In addition, also  $O_h$  (cubo-octahedron, CO) and  $D_{3h}$  (hcp) structures are perceived. Common for all of these higher-energy structures is that they can be obtained from the ICS ground state by a diffusionless mechanism where the atoms collectively twist between different isomers. The participation frequency of each isomer in the dynamics is in a qualitative accordance with the energetical ordering calculated at 0 K.<sup>21,22</sup>

Inspection of the isomerization peaks and the related geometries reveals the reason for the drastical changes in  $\text{Al}_{13}^-$  data: at first the kinetic energy of ions is not enough to drive the cluster off its more or less spherical confinement (40 valence electrons) and the cluster maps out the phase space in the vicinity of the compact geometries presented above (see also Fig. 1, isomers 1–3, 5) corresponding to a region referred to as the “soft solid;”<sup>3</sup> when more mobility is introduced the system time to time breaks off from the spheri-

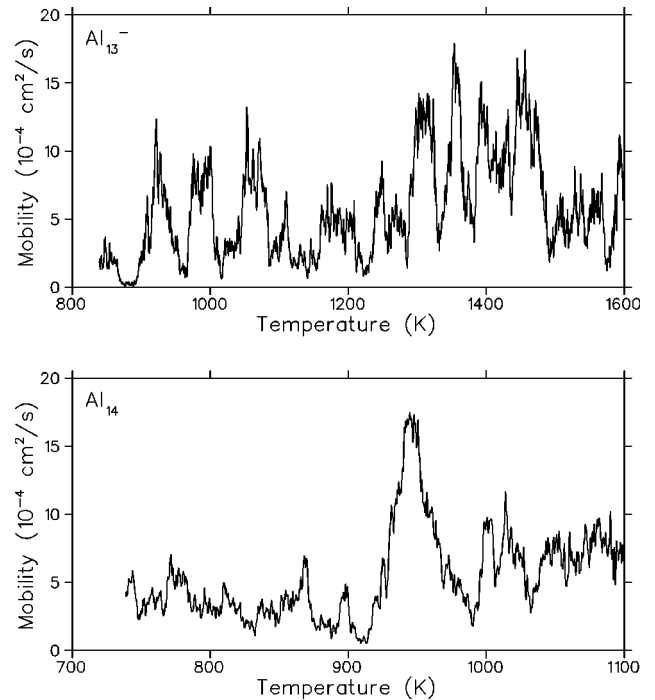


FIG. 2. The averaged atomic mobilities of  $\text{Al}_{13}^-$  and  $\text{Al}_{14}$  clusters as a function of cluster temperature. The mobilities are determined with respect to the previous time steps using a constant time separation ( $\Delta t = 3.75$  ps).

cal confinements to configurations where the potential energy is considerably higher. Indeed, some of these geometries (isomers 4, 6, and 7) could be suggested to exhibit behavior similar to floater-hole pairs, phenomenon already observed in the context of 13-atom rare gas clusters.<sup>7</sup> Furthermore, the last  $\text{Al}_{13}^-$  configuration (isomer 8) reflects a totally molten behavior evidently close to the evaporation limit.

In contrast,  $\text{Al}_{14}$  does not show isomerization peaks as strong as  $\text{Al}_{13}^-$ . The obvious reason for this is that  $\text{Al}_{14}$  does not prefer spherical confinement (42 valence electrons, ionic structure), which enables larger shape fluctuations. During the molecular dynamics we observe that the outermost atom is still the prominent feature, and increasing the kinetic energy induces additional atoms to “pop out” (see Fig. 1, e.g., isomer 8).

We further illustrate the different time evolutions of  $\text{Al}_{13}^-$  and  $\text{Al}_{14}$  clusters in Fig. 2, where we present the averaged mobilities (“diffusion constants”) of atoms as a function of temperature. The aforementioned soft solid behavior of  $\text{Al}_{13}^-$  is observed as distinct jumps in the mobility values, and while the heating does increase the mean mobility of the cluster, the peak patterns are not completely washed away. Clearly,  $\text{Al}_{14}$  exhibits a steadier pattern that is broken by one strong peak around 940 K. Further investigations of time-averaged mobilities imply that according to these single heating runs there exist gradual transitions above 1200 K and 900 K for  $\text{Al}_{13}^-$  and  $\text{Al}_{14}$ , respectively, where the clusters become more mobile.

Inspection of the mobilities of the individual atoms reveals that the atomic movements in both of the clusters can

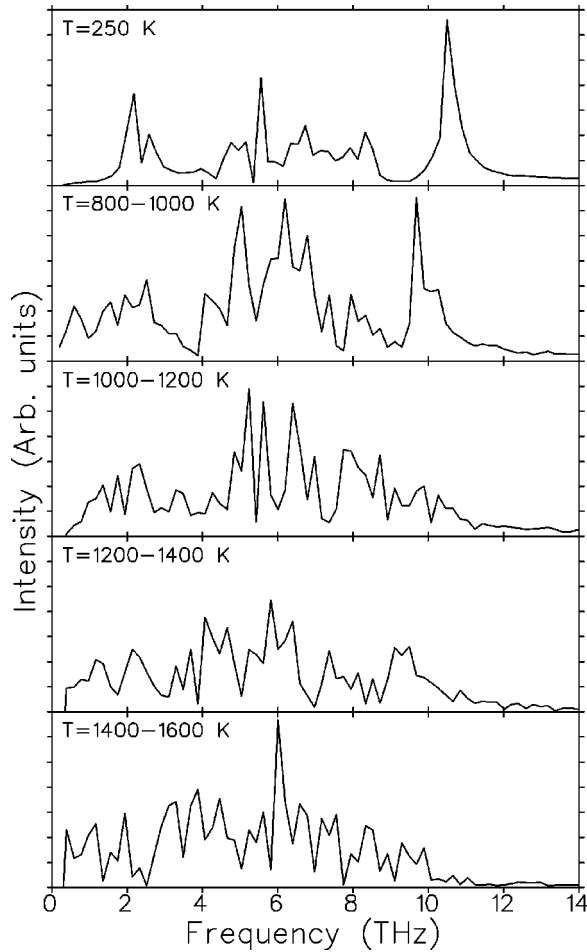


FIG. 3. The vibrational DOS of the  $\text{Al}_{13}^-$  cluster at different temperature-regimes.

be described as a collective or concerted motion, i.e., during all the significant transitions most of the atoms participate in the process. We do not see any single exchange processes where only two atoms would change places. Most interestingly, we perceive that the outermost atom in  $\text{Al}_{14}$  does not float around at any stage; instead it is frequently changed by a collective process where the “old” outermost atom inserts pushing out the “new” atom from the opposite side of the cluster. Evidently, this illustrates that for  $\text{Al}_{14}$  it is energetically more favorable to interconvert between different isomers than to float the outermost atom across the edges of the 13-atom “core” (ICS, DC, etc.). The same process is documented also for icosahedral  $\text{Ar}_{14}$  clusters as one possible transition mechanism.<sup>7</sup>

In Fig. 3 we display the vibrational density of states (VDOS) of the  $\text{Al}_{13}^-$  cluster at different temperature-regimes. The temperature-dependent VDOS are obtained as Fourier transforms (power spectra) from the corresponding velocity-velocity autocorrelation functions. The uppermost low-temperature data is from our earlier work<sup>22</sup> where the vibrating icosahedral cluster was simulated at a constant energy for 5 ps. The results in Fig. 3 can be interpreted using a simple harmonic oscillator model for atomic vibrations<sup>27</sup> where the free energy of the cluster is presented as

$$F_{\text{vib}} = V_0 + \sum_i \frac{1}{2} \hbar \omega_i + kT \sum_i \ln \left[ 1 - \exp \left( -\frac{\hbar \omega_i}{kT} \right) \right]. \quad (1)$$

Here  $V_0$  and  $\omega_i$  are the potential energy and the frequency of the  $i$ th vibrational mode, respectively. The implication of Eq. (1) is that as the temperature is increased the lower frequency modes (corresponding to relatively unstable isomers at 0 K) should become more favorable inducing a shift in VDOS towards smaller values in accordance with our simulations (see Fig. 3). Furthermore, we can see how the temperature gradually smears the spectra supporting our earlier conclusion about the gradual “melting” of  $\text{Al}_{13}^-$  above 1000 K. Similar observations can also be made from the temperature-dependent VDOS of  $\text{Al}_{14}$  (not shown) where we see clear changes in the spectra as the temperature is raised above 900 K.

According to our observations<sup>22</sup> the electronic structure and its density of states (DOS) are very sensitive to the detailed ionic geometry. Therefore, as the cluster is heated, it maps out larger and larger regions in the phase space, causing smearing and broadening effects in the DOS. This was demonstrated both theoretically and experimentally for  $\text{Al}_{13}^-$  in a recent communication by Akola et al.<sup>22</sup> where a special connection between the theoretical DOS and experimental photoelectron spectrum (PES) was employed. Here, we report further findings at a higher temperature-regime. The strong isomerization peaks of  $\text{Al}_{13}^-$  (Fig. 1) where the cluster breaks off from the compact confinements can be observed here as drastical changes in the electronic structure causing further broadening of the spectra. Especially, the highest occupied molecular orbital (HOMO) is affected, causing large drops even below 2.5 eV in the vertical detachment energy (VDE of the ICS ground state is 3.59 eV) in an excellent agreement with the wide thermal tails observed in the experimental high-temperature PES.<sup>22</sup> Furthermore, the general trend of VDE is decreasing as the temperature is raised, which we regard as a phenomenon caused by the thermal expansion of the cluster.<sup>23</sup> On the other hand, the temperature effects in the electronic spectra of  $\text{Al}_{14}$  are relatively smaller. While the KS orbital energies show considerable fluctuations, they can be assigned only weakly as temperature dependent. Especially the HOMO level of  $\text{Al}_{14}$  exhibits large fluctuations throughout the whole heating run, and the related vertical ionization potential (VIP) oscillates between 5.4 and 6.7 eV (6.46 eV for the ICS ground state), demonstrating the necessity for low-temperature conditions in experimental IP measurements.

In summary, we have studied the high-temperature behavior of  $\text{Al}_{13}^-$  and  $\text{Al}_{14}$  clusters using a first-principles simulation method. During the heating we observe strong isomerization peaks for  $\text{Al}_{13}^-$  in the potential energy curve, which are due to the strong tendency of the cluster to remain in a spherical confinement. We observe that after the bulk melting temperature (933 K) the cluster still remains in a so-called “soft solid” phase and the transition to “liquid” does not start until around 1200 K (in Ref. 28 the many-atom potential, the so-called “glue” model, gives quite a distinct melting temperature at 1400 K for  $\text{Al}_{13}$ ). Furthermore, since the restricting spherical context does not apply for  $\text{Al}_{14}$ , we

notice that its properties evolve more smoothly during the heating. We remark also that the motion in both of the clusters is very much concerted, i.e., single-atom diffusions and plain two-atom exchange processes are not supported. This is most evidently visualized by the outermost atom of  $Al_{14}$ , which sits tightly on the rest of the cluster without any floating and is constantly replaced by some other atom in a

collective process. This behavior differs drastically from the observations of corresponding rare gas clusters.<sup>6,7</sup>

This work has been supported by the Academy of Finland under the Finnish Center of Excellence Program 2000-2005 (Project No. 44875, Nuclear and Condensed Matter Program at JYFL). We want to thank J. Merikoski, H. Häkkinen, and U. Landman for valuable discussions.

\*Present address: Forschungszentrum Jülich, IFF, D-52425 Jülich, Germany.

<sup>1</sup>W.A. de Heer, *Rev. Mod. Phys.* **65**, 611 (1993).

<sup>2</sup>M. Brack, *Rev. Mod. Phys.* **65**, 677 (1993).

<sup>3</sup>R.S. Berry, in *Theory of Atomic and Molecular Clusters* edited by J. Jellinek (Springer-Verlag, Heidelberg, 1999), pp. 1–26.

<sup>4</sup>R.S. Berry and D.J. Wales, *Phys. Rev. Lett.* **63**, 1156 (1989).

<sup>5</sup>R.M. Lynden-Bell and D.J. Wales, *J. Chem. Phys.* **101**, 1460 (1994).

<sup>6</sup>T.L. Beck, J. Jellinek, and R.S. Berry, *J. Chem. Phys.* **87**, 545 (1987).

<sup>7</sup>T.L. Beck and R.S. Berry, *J. Chem. Phys.* **88**, 3910 (1988).

<sup>8</sup>I.L. Garzon and J. Jellinek, *Z. Phys. D: At., Mol. Clusters* **20**, 235 (1991).

<sup>9</sup>J. Jellinek and I.L. Garzon, *Z. Phys. D: At., Mol. Clusters* **20**, 239 (1991).

<sup>10</sup>C.L. Cleveland and U. Landman, *J. Chem. Phys.* **94**, 7376 (1991).

<sup>11</sup>S. Valkealahti and M. Manninen, *Z. Phys. D: At., Mol. Clusters* **40**, 496 (1997); *Phys. Rev. B* **57**, 15 533 (1998).

<sup>12</sup>S. Valkealahti and M. Manninen, *Phys. Rev. B* **45**, 9459 (1992).

<sup>13</sup>C.L. Cleveland, W.D. Luedtke, and U. Landman, *Phys. Rev. Lett.* **81**, 2036 (1998).

<sup>14</sup>F. Ercolessi, W. Andreoni, and E. Tosatti, *Phys. Rev. Lett.* **66**, 911 (1991).

<sup>15</sup>H.-P. Cheng and R.S. Berry, *Phys. Rev. A* **45**, 7969 (1992).

<sup>16</sup>R.E. Kunz and R.S. Berry, *Phys. Rev. Lett.* **71**, 3987 (1993).

<sup>17</sup>A. Rytönen, H. Häkkinen, and M. Manninen, *Phys. Rev. Lett.* **80**, 3940 (1998); *Eur. Phys. J. D* **9**, 451 (2000).

<sup>18</sup>M. Schmidt, R. Kusche, W. Kronmüller, B. von Issendorff, and H. Haberland, *Phys. Rev. Lett.* **79**, 99 (1997).

<sup>19</sup>H. Häkkinen and M. Manninen, *J. Phys.: Condens. Matter* **1**, 9765 (1989); *Phys. Scr.* **T33**, 210 (1990).

<sup>20</sup>H. Häkkinen and M. Manninen, *Phys. Rev. B* **46**, 1725 (1992).

<sup>21</sup>J. Akola, H. Häkkinen, and M. Manninen, *Phys. Rev. B* **58**, 3601 (1998).

<sup>22</sup>J. Akola, M. Manninen, H. Häkkinen, U. Landman, X. Li, and L.-S. Wang, *Phys. Rev. B* **60**, 11 297 (1999).

<sup>23</sup>S. Kümmel, J. Akola, and M. Manninen, *Phys. Rev. Lett.* **84**, 3827 (2000).

<sup>24</sup>R.N. Barnett and U. Landman, *Phys. Rev. B* **48**, 2081 (1993).

<sup>25</sup>N. Troullier and J. L. Martins, *Phys. Rev. B* **43**, 1993 (1991). For the aluminum  $3s^23p^1$  valence electrons, we use  $s$  nonlocal and  $p$  local components with cutoff radii of  $2.1a_0$  and  $2.5a_0$ , respectively. The KS orbitals are expanded in a plane wave basis with a cutoff of 15.4 Ry.

<sup>26</sup>S.H. Vosko, L. Wilk, and M. Nusair, *Can. J. Phys.* **58**, 1200 (1980); S.H. Vosko and L. Wilk, *J. Phys. C* **15**, 2139 (1982).

<sup>27</sup>T.P. Martin, *Phys. Rep.* **95**, 169 (1983).

<sup>28</sup>D. Y. Sun and X. G. Gong, *Phys. Rev. B* **57**, 4730 (1998).